1 *Research Article – REVISED VERSION*

2

3

4

5

6

7 **Insights into the antibacterial mechanism of action of chelating**

8 **agents by selective deprivation of iron, manganese and zinc**

9 **Joy R. Paterson,[a] Marikka S. Beecroft,[a] Raminder S. Mulla,[b] Deenah Osman,[a] Nancy**

10 **L. Reeder,[c] Justin A. Caserta,[c] Tessa R. Young,[a] Charles A. Pettigrew,[c] Gareth E.**

11 **Davies,[d] J.A. Gareth Williams,[b] and Gary J. Sharples[a]#**

12 [a]Department of Biosciences, Durham University, Durham, United Kingdom

13 [b]Department of Chemistry, Durham University, Durham, United Kingdom

14 [c]Procter and Gamble, Mason Business Centre, Cincinnati, Ohio, USA

15 [d]Procter and Gamble Technical Center Ltd, Reading, Berkshire, United Kingdom

16

17

18

19

20

21

22

23

24

25

26

27 *Running head:* Selective metal deprivation by chelating agents

28

29 KEY WORDS:chelating agents, metals, antibacterial agents, iron, manganese, zinc

30

31

32 # Address correspondence to Gary J. Sharples, gary.sharples@durham.ac.uk

33

1

ABSTRACT

Bacterial growth and proliferation can be restricted by limiting the availability of metal ions in their environment. Humans sequester iron, manganese and zinc to help prevent infection by pathogens, a system termed nutritional immunity. Commercially-used chelants have high binding affinities with a variety of metal ions, which may lead to antibacterial properties that mimic these innate immune processes. However, the modes of action of many of these chelating agents in bacterial growth inhibition and their selectivity in metal deprivation *in cellulo* remain ill-defined. We address this shortcoming by examining the effect of eleven chelators on *Escherichia coli* growth and their impact on the cellular concentration of five metals. Four distinct effects were uncovered: i) no apparent alteration in metal composition, ii) depletion of manganese alongside reductions in iron and zinc levels, iii) reduced zinc levels with a modest reduction in manganese, and iv) reduced iron levels coupled with elevated manganese. These effects do not correlate with the absolute known chelant metal ion affinities in solution, however, for at least five chelators for which key data are available, they can be explained by differences in the relative affinity of chelants for each metal ion. The results reveal significant insights into the mechanism of growth inhibition by chelants, highlighting their potential as antibacterials and as tools to probe how bacteria tolerate selective metal deprivation.

IMPORTANCE

Chelating agents are widely used in industry and consumer goods to control metal availability, with bacterial growth restriction as a secondary benefit for preservation. However, the antibacterial mechanism of action of chelants is largely unknown, particularly with respect to the impact on cellular metal concentrations. The work presented here uncovers distinct metal starvation effects imposed by different chelants on the model Gram-negative bacterium *Escherichia coli*. The chelators were studied both individually and in pairs with the majority producing synergistic effects in combinations that maximise

60   antibacterial hostility. The judicious selection of chelants based on contrasting cellular

61   effects should enable reductions in the quantities of chelant required in numerous

62   commercial products and presents opportunities to replace problematic chemistries with

63   biodegradable alternatives.

INTRODUCTION

Several transition metals are essential micronutrients for all organisms. An intricate balance of each has to be maintained to avoid deficiency or the toxic consequences of excess. Nutritional immunity, a component of the human innate immune system, makes use of the sequestration of metal ions in order to combat bacterial proliferation by starving such microorganisms of the metal ions they require (1, 2). The bioavailability of iron, manganese and zinc, in particular, is severely constrained in the human body. Bacteria attempt to counteract this host-mediated metal starvation by upregulating metal selective importers and synthesising and exporting their own chelators, such as enterobactin, to assist in metal uptake (2, 3).

Synthetic chelating agents form stable complexes with a variety of metal ions and they have the potential to mimic the metal starvation and bacterial growth restriction conditions produced by nutritional immunity. Chelants are widely used in industry, with global consumption of aminopolycarboxylates (e.g. DTPA, EDTA) alone estimated at 200,000 tonnes per annum at the beginning of the century (4). Myriad applications include water softening, effluent treatment, paper and textile manufacture, fertilizers, soil remediation, food processing, pharmaceuticals, medical detoxification, cosmetics and detergents, soaps and disinfectants employed in both industrial and domestic settings (5, 6). In many cases, chelants function as potentiators that assist preservation and thus extend the shelf life of products (7-10). Despite their importance in product formulations, the antibacterial mechanism of action of chelating agents has received little attention in recent years, with current knowledge relying on studies concentrating on the consequences for bacterial outer membrane integrity (9). Experiments with the broad-spectrum chelating ligand EDTA (ethylenediamine tetra-acetate) suggest that it damages *E. coli* by disrupting membrane permeability, possibly through the sequestration of Ca(II) and Mg(II) ions that stabilise the lipopolysaccharide (LPS) at the bacterial outer surface (9, 11-14). Treatment

4

90   of *E. coli* with EDTA enhances susceptibility to various compounds, including amines (15)

91   and antibiotics (16-19), consistent with interference with outer membrane permeability

92   (20, 21). Similar observations have been made with other Gram-negatives, including *P.*

93   *aeruginosa* (17, 22-25). Cell envelope damage by EDTA has been directly visualized by

94   atomic force microscopy of both *E. coli* (26) and *P. aeruginosa* (27). Destabilisation of

95   artificial lipid membranes has also been reported as a consequence of EDTA exposure

96   (28). Few reports have been published on the effect of any other chelants on bacteria,

97   and none appear to have examined their impact on metal homeostasis.

98   In this study, we sought to probe the effects of several different chelating ligands on

99   metal ion acquisition in the archetypal Gram-negative bacterium *E. coli*. Impetus for such

100   a study arose from the use of chelants as bacteriostatic agents in a variety of consumer

101   products and an eagerness to develop alternatives to ligands such as EDTA which largely

102   resist biodegradation (29). To this end, we have characterised the influence of eleven

103   chelants on *E. coli* growth, individually and in combination, and determined their impact

104   on total cellular metal ion concentrations. Our key objectives were to: i) identify the

105   specific metals affected by chelant exposure and their contribution to bacterial growth

106   restriction, ii) assess chelators as potential probes for metal homeostasis that mimic

107   nutritional immunity processes, iii) explore the potential of combinations of chelating

108   agents in antibacterial hostility, and iv) to begin to rationalise such observations in relation

109   to bacterial metallostasis.

110   **RESULTS AND DISCUSSION**

111   **Chelant selection and inhibitory effects on *E. coli* growth.** Eleven chelators were

112   selected based on their known or predicted metal ion affinities (30-32) and differing

113   chemical structures that might elicit a variety of complementary cellular effects (Fig. 1;

114   Table S1). Most of the chelants are commonly known by their abbreviations rather than

115   their full chemical names. The selection includes EDTA (hexadentate), its octadentate

116 analogue DTPA, and closely related biodegradable aminocarboxylates GLDA and MGDA,

117 all of which are expected to bind a broad range of metal ions strongly, especially Fe(III).

118 Metal ion affinities are quantified in terms of stability constants (association constants),

119 namely the equilibrium constant K_A for the equilibrium M + L $\rightleftharpoons$ ML at a given pH, ionic

120 strength and temperature, typically expressed as log K_A. Where available, log K_A values

121 for the selection of chelants used in this study for a number of biologically relevant divalent

122 cations in combination with Fe(III) are listed in Table S1. The metal ion affinities of GLDA

123 and MGDA (29) are lower than those of DTPA and EDTA (Table S1), indicating that higher

124 concentrations may be required to chelate biologically relevant metal ions. DTPMP has a

125 similar nitrogenous backbone to DTPA but possesses five pendant phosphonates –

126 P(O)(OH)$_2$ instead of carboxylates –C(O)OH. HBED is another aminocarboxylate, but it

127 also incorporates phenolic units that favour binding to Fe(III) (31, 33). Catechol (CAT; a

128 unit that occurs in enterobactin) has very high selectivity for Fe(III) *in vitro* (34), although its

129 effective binding strength at pH 7 is attenuated due to competitive protonation. CHA is a

130 simple hydroxamate that resembles the constituent binding units of the siderophore

131 desferrioxamine, which binds Fe(III) extraordinarily strongly (35). Piroctone (the metal

132 binding unit of piroctone ethanolamine, PO) is a related cyclic hydroxamate. TPEN and

133 BCS are "softer" ligands that favour binding to late transition metals such as Zn(II) (36) and

134 Cu(I) (37), respectively.

135 The effect of each of the 11 chelants on bacterial growth was evaluated using 2-fold

136 serial dilutions of each ligand (Fig. 2). The *E. coli* K-12 strain BW25113 was chosen to

137 allow comparisons with deletion mutants from the Keio collection, a comprehensive set of

138 single-gene knockout mutants (38). LB (Lennox) broth was selected as the growth

139 medium, as it is widely used in cultivation of *E. coli* and offers good reproducibility. The

140 provision of a rich growth medium with no inorganic nutrient restrictions (39) allowed an

141 assessment of sensitivity to chelants when bacteria are in a robust physiological state.

142 Bacterial growth was evaluated based on the optical density at 600 or 650 nm after

143 incubation with the chelant(s) for 16 h as in minimum inhibitory concentration (MIC)

144 determination assays (40). One of the chelants tested, BCS, failed to inhibit bacterial

145 growth fully even at the highest concentrations tested (Fig. 2). The dose-response curves

146 with different chelants also varied, with several chelants (CAT, CHA, GLDA, MGDA and

147 PO) exerting little effect on growth until a particular threshold concentration was reached.

148 Others (DTPA, DTPMP and EDTA) resulted in higher susceptibility at low chelant

149 concentrations and produced a correspondingly linear reduction in growth (Fig. 2). These

150 different sensitivity profiles could be an indication of dual antibacterial effects, such as

151 metal starvation coupled with membrane permeabilization, invoked previously as an

152 explanation for the biphasic inhibition profile of EDTA with *P. aeruginosa* (8). DTPA and

153 EDTA share similar molecular structures (Fig. 1) that may correspond to an analogous

154 mechanism of growth inhibition. In most cases, high concentrations were required to

155 achieve *E. coli* growth inhibition of >90%. To validate these findings, the experiments were

156 repeated with the chemically-defined MOPS-minimal medium supplemented with glucose

157 as the sole carbon source (41). In general, a similar pattern of effects was observed in

158 comparison with the more complex LB broth (Fig. S1). The minor changes seen with BCS,

159 HBED and TPEN may reflect differences in the quantities or relative proportions of the

160 metals present in each medium (see below). The MICs were also similar (Fig. 2), although

161 6-fold less CAT and 10-fold less EDTA were required to inhibit the growth of *E. coli* in the

162 minimal medium relative to LB. The two chelants with highest efficacy in both media were

163 PO and TPEN with MICs of 75 and 400 µM in LB and 250 and 200 µM in MOPS-minimal

164 media, respectively (Fig. 2). PO activity is, however, ambiguous owing to it being

165 comprised of two components. We separated the piroctone from the ethanolamine and

166 found that the former induced growth inhibition comparable to PO, whereas the latter was

167 around 500-fold less active (Fig. S2). Thus, it is the piroctone fragment that is functionally

7

168 active in bacterial growth reduction, and its activity can reasonably be attributed to its

169 chelating ability.

170 The concentration of metal ions in the LB (Lennox) medium used was determined by

171 inductively-coupled plasma mass spectrometry (ICP-MS; Fig. S3) to provide insight into

172 availabilities prior to examining the effect of chelants on cellular metal content. The metal

173 composition corresponds well with estimates from previous studies using LB (Miller) broth

174 (Fig. S3) (42, 43). The metal content of MOPS-minimal medium was also analysed and

175 found to contain 3.5-fold more magnesium and 2.4-fold more iron, but 19.5 times less

176 calcium than LB (Lennox). Interestingly, the levels of zinc were below the threshold of

177 detection (Fig. S3), although these low concentrations are not likely to be limiting for *E. coli*

178 (44).

179 **Total cellular metal content of *E. coli* exposed to metal chelators.** In order to probe

180 the effect of chelants on cellular metal composition we exposed *E. coli* to concentrations of

181 each ligand that resulted in 10-15% growth inhibition in mid-log phase in LB (Lennox)

182 media. Modest growth inhibition rates were chosen to avoid cellular damage that could

183 potentially skew metal content measurements, owing to increased permeability or cell

184 death. In addition, growth reductions at such low chelant concentrations can be

185 reasonably correlated with cellular metal deprivation. It should be noted that chelating

186 agents that associate with the envelope or reach the cytosol could sequester metals but

187 these cannot be differentiated from the bioavailable metals also present within the cell.

188 Hence, any decreases detected in cellular metal content must be primarily caused by

189 depletion of metals from the extracellular environment or from the bacterial exterior

190 surface. The total number of calcium, iron, magnesium, manganese and zinc ions in each

191 cell was determined using ICP-MS. Copper was also measured but its low concentration

192 made determination less accurate and more prone to variation. Analysis of cobalt and

193 nickel was not undertaken due to the extremely low levels present in *E. coli*. Cobalt is not

8

194 required by *E. coli* (45) and nickel is only utilised by a small number of [NiFe] hydrogenase

195 isozymes (46). Bacteria were grown in the presence of each chelant, harvested in mid-

196 exponential phase and the total cellular metal composition, expressed in atoms per cell,

197 was determined relative to controls in the absence of the chelant (Fig. 3 and Table S2).

198   Four distinct categories of effect on cellular metal content were identified, primarily

199 through differential effects on zinc, iron and manganese concentrations (Fig. 3), and the

200 results are discussed below according to these functional groupings. It is notable that

201 cellular levels of calcium or magnesium were largely unaffected by exposure to each of the

202 ligands.

203   **(i) No apparent effect on cellular metal content – BCS, CAT and CHA.** The results

204 with BCS, CAT and CHA were unexpected in that they showed no significant impact on

205 the metal composition of *E. coli* cells (Fig. 3; Table S2); these chelants also had no effect

206 on copper levels, although the results with BCS were highly variable (Table S2). Either

207 they act by a completely different mechanism to restrict bacterial growth (i.e. not involving

208 the perturbation of metal availability) or, perhaps more likely, they sequester metals within

209 the cell making them inaccessible to the proteins that require them for functionality. This

210 could potentially occur at the inner or outer membrane, the periplasm or in the cytosol,

211 depending on whether the chelator can traverse the cell wall barrier. It is suggested that

212 chelant-membrane interaction might be more likely in these cases, based on the

213 lipophilicity of these ligands, as reflected by estimations of their partition coefficients in

214 their most likely ionisation states at neutral pH. For example, the long hydrophobic tail and

215 polar head in CHA could potentially insert into the outer membrane and thereby trap

216 essential metals at the surface so they cannot gain access to the cell.

217   **(ii) Decreased manganese, iron and zinc – DTPA, EDTA, GLDA and MGDA.** The

218 principal effect of the azacarboxylate ligands DTPA, EDTA, GLDA and MGDA at 10-15%

219 growth inhibition is to deplete *E. coli* of manganese, with the reductions ranging from 5- to

9

220 15-fold relative to untreated controls (Fig. 3; Table S2). Zinc concentrations were also

221 reduced at relatively low concentrations of each of these chelants (Fig. 3; Table S2). The

222 total cellular content of iron was also lowered with DTPA, EDTA and GLDA, but not

223 significantly with MGDA (Fig. 3; Table S2). Small reductions in calcium levels were

224 apparent with EDTA and GLDA. The preferential targeting of manganese is surprising

225 given that these chelants would be expected to show a clear preference for iron based on

226 log K_A values (Table S1). There are a number of manganese-dependent enzymes in *E.

227 coli* that could be rendered inactive by manganese starvation, including Mn-superoxide

228 dismutase SodA (47), Mn-dependent ribonucleotide reductase NrdEF (48) and the haem

229 biosynthetic enzyme coproporphyrinogen III oxidase HemF (49). Mismetallation of these

230 enzymes (45, 50) and loss of the antioxidant properties of manganese could result in cells

231 being more prone to damage by reactive oxygen species (51). However, low levels of

232 manganese are not problematic for *E. coli* cells unless iron is scarce or they are exposed

233 to hydrogen peroxide (52). Hence, the additional reductions in iron and zinc, alongside

234 manganese depletion, likely impact on multiple metabolic systems and disrupt

235 compensatory pathways for metal import (see below). We investigated this further by

236 supplementing cultures with manganese chloride in the presence of EDTA (Fig. S4). Both

237 EDTA and Mn(II) cause *E. coli* growth inhibition in a concentration-dependent manner (Fig.

238 S4A and B). When EDTA and Mn(II) are mixed at different ratios, improved growth was

239 observed (Fig. S4C and D) consistent with reversal of the cellular manganese deficiency.

240 However, this response could simply be a consequence of EDTA-Mn(II) association in the

241 medium, with the complexes formed moderating the adverse effects associated with EDTA

242 metal sequestration. Supplementation of EDTA-treated *P. aeruginosa* and *S. typhimurium*

243 cells with Ca(II) and Mg(II) has been previously reported (7, 17, 21, 53), with the positive

244 effects attributed to either membrane stabilisation or alleviation of the detrimental EDTA

245 excess by chelant-metal binding.

246 **(iii) Decreased iron and elevated manganese – DTPMP, HBED and PO.** DTPMP,

247 HBED and PO affect cells similarly to one another, reducing cellular iron concentration

248 coupled with a substantial *increase* in manganese (Fig. 3; Table S2). There was no

249 significant change in levels of calcium, magnesium or zinc (Fig. 3). *E. coli* cells are known

250 to import manganese as a cellular response to iron starvation (45, 52). Manganese-

251 equivalents of iron-redox enzymes, e.g. Mn-superoxide dismutase (47, 54) and Mn-

252 dependent ribonucleotide reductase (48), can substitute for iron-containing equivalents,

253 while manganese can functionally substitute for iron in many mononuclear iron enzymes

254 (45, 55). Iron and manganese metal homeostasis systems are linked *via* the ferric uptake

255 regulator (Fur) and the proton-dependent manganese importer MntH (56). The *E. coli* Fur

256 protein, when complexed with Fe(II), represses the expression of a suite of genes involved

257 in iron uptake, metabolism and bacterial virulence (57, 58). Thus, when iron levels are

258 limiting, the affinity of Fur for its promoter sites is reduced leading to upregulation of the

259 iron homeostasis network. One such gene negatively regulated by Fur-Fe(II) is *mntH*, in

260 accordance with the cellular response that switches to manganese import when iron is

261 scarce (56, 59). The manganese superoxide dismutase (MnSOD) is similarly negatively

262 regulated by Fur-Fe(II), whereas Fur-Fe(II) activates expression of iron superoxide

263 dismutase, FeSOD (60, 61). Hence, as iron levels in the cell decrease, FeSOD levels

264 decline just as MnSOD levels rise, concomitant with increased manganese uptake. The

265 decreased levels of iron combined with increased manganese induced by DTPMP, HBED

266 and PO can reasonably be explained by bacterial adaptation to protect against iron

267 starvation.

268 To further investigate the contrasting effects of PO and EDTA on cellular iron and

269 manganese levels, we examined expression of the manganese importer by monitoring β-

270 galactosidase activity from a reporter strain, SIP879, carrying an *mntH-lacZ* fusion (59).

271 Interpretation of the experimental data is complicated by the fact that *mntH* is regulated by

11

272   both MntR, the manganese regulator, and Fur so we also tested a strain, SIP943, that

273   lacks both *mntH* and *mntR* (59). MntR is a repressor of *mntH* promoter activity under

274   manganese replete conditions (59, 62). Treatment of SIP879 with PO induced expression

275   of the *mntH-lacZ* promoter (Fig. S5A), a typical cellular response to iron starvation (59,

276   62). Similar expression levels between the *mntH-lacZ* and *mntH-lacZ mntR* strains

277   exposed to PO (Fig. S5A) is also consistent with this being a Fur-mediated response to

278   iron deprivation. Hence, iron restriction by PO would be expected to trigger manganese

279   import by MntH, corroborating earlier findings (Fig. 3). The experiments were repeated

280   with EDTA (Fig. S5B) as a representative of chelants that severely restrict cellular

281   manganese concentration, alongside reductions in iron and zinc (Fig. 3). Interestingly,

282   EDTA treatment resulted in activation of *mntH* (Fig. S5B), producing similar effects to PO

283   and indicating that both chelants deprive cells of iron. As with PO, the levels of *mntH*

284   expression were largely unaffected by the absence of *mntR* (Fig. S5B). EDTA has

285   previously been reported to induce expression of *mntH* in both *E. coli* (59) and *Salmonella*

286   (62). Thus, we can conclude that *E. coli* is subjected to iron starvation following exposure

287   to EDTA. However, unlike the situation with PO, the cells are unable to switch to their

288   regular recovery pathway because EDTA has also effectively removed access to

289   manganese.

290   The effect of EDTA on bacterial growth following manganese chloride supplementation

291   (Fig. S4) was revisited in experiments with the *mntH-lacZ* fusion (Fig. S5C). Inclusion of

292   additional manganese to cells growing in LB broth did not induce expression from the

293   *mntH* promoter as expected since MntR-mediated repression is only alleviated by

294   manganese limiting conditions (59, 62). Increased *mntH-lacZ* expression by EDTA was

295   reduced by addition of manganese chloride, especially at equimolar concentrations (Fig.

296   S5C). Similar results were obtained with SIP943, although lower levels of β-galactosidase

297   activity were detected in response to EDTA in all of these experiments (Fig. S5C). While it

298   is difficult to distinguish improvements in chelant tolerance due to either Mn(II) uptake by

299   cells or removal of chelant toxicity by Mn(II) sequestration in the medium (Fig. S4), the

300   absence of activation of *mntH-lacZ* when EDTA and Mn(II) are mixed in equal quantities

301   argues in favour of the latter.

302   **(iv) Decreased zinc and manganese – TPEN.** The predominant effect of TPEN is on

303   zinc concentration, consistent with its known affinity for Zn(II) (36), although as with the

304   other chelants it will bind a range of other metals (Table S1). At higher concentrations of

305   TPEN, manganese levels are also slightly reduced and may contribute to growth inhibition

306   by TPEN (Fig. 3; Table S2). However, at 300 µM TPEN there is no reduction in Mn(II)

307   whereas Zn(II) is reduced (1.5-fold). These results indicate that even relatively small

308   reductions in cellular zinc levels may adversely affect *E. coli*, in keeping with earlier

309   findings using zinc-depleted media (44). Microarray analysis of *E. coli* exposed to TPEN

310   (63) links chelant exposure with increased expression of genes regulated by the zinc

311   uptake regulator (Zur) (64) but also those controlled by Fur, implying that TPEN may not

312   be entirely selective for zinc. TPEN is often referred to as a membrane-permeable chelator

313   and has been reported to enter *E. coli* cells (36). Preferential removal of zinc from the

314   extracellular environment can account for the reductions in cellular zinc observed here, but

315   it is likely that intracellular zinc is also sequestered by TPEN and contributes to bacterial

316   growth inhibition.

317   **Effect of chelant combinations on *E. coli* growth.** To gain further insight into the

318   impact on bacterial metal restriction, pairs of chelants were tested based on the

319   supposition that those affecting different metal uptake pathways should be synergistic

320   when combined. The checkerboard, or 2-dimensional, assay provides a simple way to

321   evaluate inhibitory interactions between two soluble compounds and has been widely used

322   to compare efficacies of different antibiotics in combination. The microdilution method used

323   for our MIC assays was adapted with consideration of published protocols for the

13

324   interpretation of checkerboard results (65, 66). The use of checkerboard assays is

325   complicated with chelating agents because in some cases, bacterial growth is never fully

326   inhibited, unlike with many antibiotics. For instance, BCS at a maximal concentration of

327   100 mM only inhibits *E. coli* growth by 70-80% (Fig. 2). A percentage growth of <10% was

328   chosen as a baseline for minimum inhibitory concentrations, which are needed to calculate

329   a fractional inhibitory concentration (FIC) index. For cases like BCS where <10% growth

330   was not achieved, the maximum concentration of chelant provided the MIC and should be

331   taken into account when assessing results obtained with BCS. Representative examples

332   of synergistic, indifferent (or non-interacting) and antagonistic pairings from our studies are

333   illustrated in Figure 4A-C. Overall 55 chelant pairings were tested and FIC indices

334   determined (Fig. 4D), revealing one antagonistic, 26 indifferent and 28 synergistic

335   combinations by selecting the lowest possible combination of each chelant in cumulative

336   calculations (Supplemental Material Data File S1). Considerably fewer synergistic pairings,

337   only 5 (plus 8 mixed synergistic/indifferent outcomes), were obtained using an average

338   FIC method, although that is not surprising as such an approach employs much stricter

339   criteria for assigning synergy (67) (Fig. S6). Synergistic, indifferent and antagonistic

340   pairings are listed according to their effect on metal content to facilitate comparisons

341   between groups (Fig. S7). DTPA yielded the highest number of synergistic pairings, with 9

342   partners (Fig. 4 and S7). BCS produced the lowest number, displaying synergism only with

343   DTPA (Fig. S7), perhaps because of its limited capacity to fully inhibit bacterial growth

344   (Fig. 2 and Supplemental Material Data File S1).

345   **Comparison of checkerboard and metal composition data.** We predicted that

346   chelant categories that cause similar effects on cellular metal levels would produce

347   indifferent outcomes when combined. Conversely, those with dissimilar effects on metal

348   composition might be expected to yield synergistic results. To some extent this proved to

349   be the case, but there were notable exceptions (Fig. 4 and S7). Although the majority of

14

350 the synergistic pairs do indeed match complementary categories of metal deprivation,

351 there are 7 examples (DTPA/GLDA, DTPA/MGDA, DTPMP/HBED, DTPMP/PO,

352 EDTA/GLDA, EDTA/MGDA and GLDA/MGDA) where chelants individually induce

353 analogous cellular responses to metals yet produce synergistic effects in combination.

354 There are also multiple examples of chelants from the different metal effect categories

355 defined earlier that show indifference (e.g. DTPMP/EDTA, GLDA/HBED, MGDA/TPEN).

356 The results suggest that there are several different ways that chelants function in depriving

357 cells of metals, even for those that appear to have the same overall effect. Preferential

358 removal of metal either from the media or at the bacterial surface as a function of chelant

359 structure may account for some of these differences. Alternatively, there may be effects

360 produced by chelant-metal association at membranes or in the cytosol that influence metal

361 accessibility. It is interesting to note that CAT and CHA display an identical pattern of

362 synergistic and indifferent outcomes with 7 other chelants and are also indifferent with

363 each other (Fig. S7). These findings suggest that CAT and CHA are functionally equivalent

364 in depriving cells of the same subset of metals despite their dissimilar structures (Fig. 1).

365 This is informative since neither of these chelants appeared to affect total cellular metal

366 content (Fig. 3).

367   Phenolic compounds, such as CAT, are known to form brown complexes with Fe(III)

368 with absorbance between 380-800 nm (68) and this was apparent when CAT was mixed

369 with media in the presence (Fig. S8A) or absence (Fig. S8B) of bacteria. Different chelant

370 combinations with CAT exacerbated or alleviated the formation of these coloured

371 complexes (Fig. S8A). Those chelants that deprive cells of iron (Fig. 3), such as HBED

372 and PO, appear to reduce the formation of this complex as judged by a loss of colour. In

373 contrast, those predominantly affecting manganese, such as EDTA and GLDA, promote

374 the formation of the dark brown colour (Fig. S8A). The comparatively high concentrations

375 of these chelants, coupled with their relative affinities for different metals, likely serves to

15

376 remove competing metals from the media, thereby making iron more available for

377 sequestration by CAT. Depending on their commercial application, certain chelant

378 combinations might be best avoided because of the production of pigment, although at

379 lower concentrations this may not be problematic.

380 TPEN is synergistic with all but four chelants (BCS, EDTA, GLDA and MGDA),

381 indicating that reductions in cellular zinc levels might be highly effective as a means of

382 restricting bacterial growth when combined with chelants that primarily limit the availability

383 of other metals. Four chelant pairings (DTPA/DTPMP, DTPA/HBED, DTPA/PO and

384 EDTA/PO) that mainly reduce manganese or iron levels produce synergistic outcomes,

385 although many more chelants from these two categories do not (Fig. 4 and S7). Membrane

386 damage associated with EDTA (9, 14, 20), and potentially with the structurally-related

387 DTPA, may serve to drive partner chelants across the bacterial outer membrane and allow

388 targeting of the periplasm or cytosol. This might account for DTPA/GLDA and EDTA/GLDA

389 synergism, despite all three having similar effects on deprivation of cellular manganese,

390 zinc and iron. In addition, some chelants (e.g. HBED, PO) are somewhat lipophilic and

391 could associate better with membranes, particularly if the LPS layer is damaged. This fits

392 with the iron-binding ligands PO and HBED being synergistic with the hydrophilic DTPMP,

393 another iron chelator (Fig. 4 and S7). Hence the effect of metal starvation coupled with

394 membrane damage or penetration could be instrumental in the bacterial growth restriction

395 phenotype seen with these chelating agents.

396 **Analysis of bacterial metal content with chelants in combination.** To further

397 understand how chelant combinations exert synergistic effects, we selected two

398 synergistic pairs, DTPA/PO and DTPMP/PO, which show distinct effects on cellular metal

399 composition. A fixed concentration of the first chelant producing ~10% bacterial growth

400 inhibition was employed with increasing amounts of the second chelant to produce a 10-

401 30% final growth restriction. As before, the cellular levels of calcium, iron, magnesium,

16

402   manganese and zinc were determined using ICP-MS (Fig. 5). Selected results showing the

403   proportional change in metal content from experiments with PO in combination with either

404   DTPA or DTPMP are also shown in Table S3.

405   DTPA and PO have a radically different impact on the metal composition of *E. coli* and

406   function as a highly synergistic pair (Fig. 4); DTPA depletes cells of manganese, alongside

407   reductions in iron and zinc, whereas PO increases manganese in response to iron

408   limitation (Fig. 3). We predicted that synergy might be due to DTPA preventing the influx of

409   manganese induced by PO. However, the results showed that the effect of PO seems to

410   dominate over that of DTPA, yielding results similar to PO alone (Fig. 5A; Table S3).

411   Modest increases in calcium were evident at a few concentrations of both chelants (Fig.

412   5A), but there were no significant changes in other metals comparing PO alone with the

413   PO-DTPA combination. As suggested above, the potential influence of DTPA on

414   membrane integrity could exacerbate the activity of the lipophilic PO.

415   In contrast to the DTPA/PO pairing, DTPMP and PO behave similarly in reducing levels

416   of iron and increasing manganese, yet display a synergistic effect on *E. coli* growth where

417   an indifferent response was anticipated. There was little change in metal levels between

418   the effect of DTPMP alone and samples that combined DTPMP with increasing amounts of

419   PO, apart from some reduction in zinc at lower PO concentrations (Fig. 5B; Table S3). It

420   should be noted that a small, but significant, reduction in zinc was evident with DTPMP

421   (Fig. 5B) that was not detected previously with this chelant (Fig. 3). To probe this further,

422   the reciprocal experiment was performed using a fixed concentration of PO and titration of

423   DTPMP (Fig. 5C; Table S3). In this case, a significant reduction in zinc was evident at all

424   concentrations of both chelants relative to PO alone. Although the results are not

425   statistically different due to variability in the data sets, there was also a consistent

426   decrease in iron and increase in manganese when the chelants were combined (Fig. 5C,

427   compare the symbols for each data set). These results are in keeping with DTPMP and

17

428 PO producing the same effects on cellular levels of manganese and iron, but an additional

429 reduction in zinc when combined. This latter effect may be responsible for the synergism

430 observed between these two chelants (Fig. 4).

431 **Effect of PO on the growth of *E. coli* mutants from the Keio collection.** To provide

432 insight into the gene products important for tolerating exposure to chelants we next

433 selected one of the iron chelators, PO, in a screen of the *E. coli* Keio collection of single

434 gene deletions to identify mutants with increased susceptibility. The duplicate set of the

435 Keio collection of 3985 mutants (7970 strains in total) was cultivated in 96-well plates in LB

436 media in the presence of low levels of PO at 27 and 34 μM. The growth of each strain

437 exposed to PO relative to untreated controls was determined after overnight incubation

438 and the most sensitive mutants identified (Fig. 6A; Supplemental Material Data File S2).

439 The influence of EDTA on *E. coli* growth has previously been analysed by inoculating the

440 Keio collection mutants onto LB agar plates (69) and this facilitated comparisons with our

441 data on PO (Fig. 6B). The Keio screen with PO highlighted the importance of genes

442 involved in iron-siderophore uptake for PO tolerance (Fig. 6C). Mutants affecting

443 enterobactin synthesis (Aro, Ent), export (TolC) and import (FepA-G, ExbBD-TonB and

444 Fes) were among those with the most substantial growth reductions relative to the control

445 following PO exposure (Fig. 6A and 6C). Deletion mutants affecting envelope integrity,

446 efflux pumps, damage tolerance and stress responses also showed sensitivities to PO

447 (Fig. 6A), potentially indicating that PO can more readily gain access to the periplasm or

448 cytosol in these strains and thereby affect growth. Some similarities in growth behaviour

449 with EDTA (69) were observed with a similar subset of genes involved in enterobactin-iron

450 uptake and membrane integrity affected. However, unlike PO, mutants defective in

451 components of the Znu zinc uptake system showed impaired growth when exposed to

452 EDTA (Fig. 6B).

18

453   A small number of mutants displayed improved growth relative to untreated controls

454   when PO was incorporated in the growth medium (Table S4). Several of these mutants

455   display better growth at both PO concentrations suggesting that their deletion does

456   correspond to a genuine improvement in growth. These mutants correspond to genes

457   linked to regulatory pathways, metabolic processes and repair of oxidative damage.

458   However, the largest group of mutants affected are those engaged in flagellar

459   biosynthesis, of which 26 *fli*, *flg* and *flh* genes occur in the 200 mutants that show the most

460   enhanced growth at both PO concentrations (Table S4). This may represent an alleviation

461   of the substantial energy cost involved in flagellum assembly and operation (70) during the

462   iron limitation imposed by PO. Significantly, flagellar gene-deficient mutants do not exhibit

463   the most enhanced growth of the Keio mutant strains under low iron conditions using

464   MOPS media (69) suggesting that PO either exerts additional detrimental effects or targets

465   iron depletion with a different cellular specificity.

466   **Effect of PO, EDTA and DTPMP on the growth of selected *E. coli* Keio collection**

467   **mutants.** To validate the findings with the Keio screen, we selected a range of the most

468   PO susceptible mutants and others deficient in related iron, manganese and zinc uptake

469   pathways for further testing. All of the mutants affecting enterobactin biosynthesis or

470   uptake (*aroA*, *fepA*, *fepC* and *fes*) (71) exhibited substantially reduced growth relative to

471   the wild-type following exposure to PO (Fig. 7A), consistent with the importance of iron

472   acquisition for tolerance of this chelant. Interestingly, a corresponding sensitivity was not

473   found with *fepB* and *fepD* mutants (Fig. S9A). Several strains lacking integral membrane

474   proteins involved in drug export and envelope integrity (*acrB*, *envC* and *tolC*) also showed

475   some increased susceptibility as in the Keio screen with PO (Fig. 7A). Two mutants, *znuB*

476   and *znuC,* affecting zinc import (72) behaved similarly to the wt as expected. Mutants

477   affecting components of the Fe(III)-citrate (*fecA*, *fecB*, *fecD* and *fecE*) and Fe(III)-

478   hydroxamate (*fhuF*) systems (73) were generally no more susceptible to PO. Similarly,

19

479   mutants involved in cysteine (*cysE*) and histidine (*hisI*) biosynthesis that are highly

480   sensitive to iron starvation (69), showed no increased susceptibility to PO (Fig. S9A).

481   The same strains were also examined for their susceptibility to DTPMP and EDTA (Fig.

482   7B and 7C), the latter allowing comparisons with published data (69) that were conducted

483   on solid rather than liquid media. As with PO, defects in the enterobactin pathway (*aroA*,

484   *fepA*, *fepC* and *fes*) produced the highest sensitivity to these two chelants, underlining the

485   necessity of this route of iron acquisition for bacterial growth and defence against these

486   chelants. In contrast to PO, the other ferric iron import pathway mutants also showed

487   increased susceptibility, especially with DTPMP (Fig. S9B and S9C). Reduced growth

488   following chelant exposure was apparent with mutants affecting membrane integrity

489   functions.

490   Mutants in the *znuB* and *znuC* zinc import system were much more sensitive to DTPMP

491   and EDTA (Fig. 7B) than PO (Fig. 7A), suggesting that reductions in cellular zinc – either

492   due to mutation or sequestration by a ligand such as TPEN – increase chelant

493   vulnerability. DTPMP treated cells display low levels of iron and elevated concentrations of

494   manganese (Fig. 3), however, small reductions in zinc were also apparent, especially

495   when combined with PO (Fig. 5B). The enhanced susceptibility of *znu* mutants to DTPMP

496   but not PO indicates that these two chelants do not behave precisely in the same way and

497   that additional effects on zinc may account for their synergistic behaviour (Fig. 4). Deletion

498   of the manganese importer, MntH, did not result in decreased growth following EDTA

499   exposure (Fig. S9C) in agreement with previous studies (69). In repeat assays, growth

500   was actually improved following EDTA treatment in an *mntH* strain (Fig. S10). Although it

501   is not clear why growth would be improved in the absence of *mntH*, these observations are

502   consistent with combined reductions in iron, manganese and zinc, rather than manganese

503   alone, being important for bacterial growth inhibition by EDTA.

504   **CONCLUSIONS**

20

505   Using *E. coli* as a model organism, the specific metals affected by a selection of chelating

506   agents have been identified and their impact on bacterial growth and metal deprivation

507   evaluated. The cellular concentrations of calcium, iron, magnesium, manganese and zinc

508   were determined for eleven chelators with differing structures and metal ion selectivities.

509   Four categories of chelants with distinct effects on metal depletion were identified.

510   BCS, CHA and CAT do not appear to alter the levels of any of the metals tested,

511   although it is possible that they trap particular metals, potentially at the cell surface, and

512   thus prevent metals from accessing the cell. Hence the metals would remain associated

513   with the cell but would be unavailable to essential intracellular enzymes. Of these three,

514   CHA and CAT appear to be functionally equivalent as judged by their similar behaviour in

515   combination with other chelants.

516   DTPA, EDTA, GLDA and MGDA all produce a dramatic decrease in cellular

517   manganese, combined with lesser reductions in both iron and zinc. Iron and zinc limitation

518   could well be the principal factor in bacterial growth inhibition with these chelants since *E.*

519   *coli* mutants with defects in uptake pathways for these metals (e.g. *fepA*, *fes*, *znuB*) are

520   more sensitive to EDTA (Fig. 6 and 7) (69). That manganese has only a secondary effect,

521   perhaps at the cell surface, fits with the improved growth of an EDTA-treated *mntH* mutant

522   (Fig. S10), which lacks the MntH manganese transporter that would boost cytosolic levels

523   of Mn(II) (55). Examination of *mntH* promoter activity (Fig. S5) confirmed that EDTA

524   starves cells of iron, but is also likely to prevent manganese import by sequestration

525   making this route of tolerance ineffective. EDTA, and potentially DTPA, has known

526   detrimental effects on outer membrane integrity (9, 27), meaning that a combination of

527   metal starvation and membrane damage likely contributes to its antibacterial mechanism

528   of action. It is feasible that stripping of manganese from a primary location at the bacterial

529   surface is responsible for the injurious effects on membrane stability. The cellular location

21

530   of manganese has yet to be established (55), although in the Gram-positive *Bacillus*

531   *subtilis,* Mn(II) does appear to be associated with the cell wall (74).

532   Exposure of *E. coli* to DTPMP, HBED and PO causes a reduction in iron and an influx

533   of manganese; the triggering of manganese import is a known cellular defence response

534   to iron starvation (45, 52) in keeping with these ligands being Fe(III) chelators.

535   Experiments with combinations of these three chelants, however, suggest that they are not

536   functionally equivalent and that their cellular targets may differ. Cells deficient in the zinc

537   (Znu) uptake and ferric-citrate (Fec) pathways are hypersensitive to DTPMP but not PO

538   (Fig. 7 and S9) and reductions in cellular zinc levels were apparent with DTPMP,

539   especially when mixed with PO (Fig. 5). As with DTPA, EDTA, GLDA and MGDA, the

540   potential for membrane penetration or damage may account for the differing interactions

541   observed.

542   Why might certain chelants, such as EDTA and DTPA, deplete cells of manganese

543   considerably more than iron? Affinities for both Fe(III) and Mn(II) are known for five of the

544   chelants which interfere with the accumulation of these metals, namely DTPA, EDTA,

545   GLDA, HBED and MGDA (Table S1). Figure 8 shows their relative affinities (as

546    $\log(K_{Fe(III)}:K_{Mn(II)})$ where K_{metal} correspond to association constants K_A) along with

547   comparative estimated values for uptake systems for these two metals: note that an

548   available $K_{Mn(II)}$ from *S. aureus* MntC has been used in the absence of a measured value

549   for *E. coli* MntH, and a pseudo-K_A for Fe(III)-citrate$_2$ was simulated for defined total Fe(III)

550   and citrate concentrations (1 µM and 100 µM, respectively; (75)). Importantly, only

551    $\log(K_{Fe(III)}:K_{Mn(II)})$ for HBED exceeds estimated values for all uptake systems (Fig. 8), and

552   of the five chelants only HBED impairs the uptake of iron and not manganese (Fig. 3).

553   Thus, even if two chelants show tightest affinity for the same metal, their relative affinities

554   (for different metals) can drastically alter their impact on cellular metal acquisition systems.

555   This preliminary analysis suggests that it may be possible to model bacterial responses to

556   chelants based on relative metal affinities and by measuring K_A for all uptake systems for

557   all metals to predict cellular responses to chelants.

558   As outlined above, analysis of the cellular metal selectivity of the chelants tested

559   allowed the identification of chelants with high specificity for iron, manganese and zinc that

560   could serve as mimics of nutritional immunity and as tools to probe bacterial metal

561   homeostasis. Those with specificity for zinc and iron offer clear value although those

562   affecting manganese may exhibit too broad a range of metal target. There is considerable

563   potential to exploit two, or even three, chelants to restrict bacterial growth in a range of

564   consumer, industrial and healthcare settings. For example, CHA, EDTA and PO acting by

565   different mechanisms could prove a potent antibacterial mixture. Chelators could be

566   deployed in combination with antibiotics for wound care and other therapeutic applications,

567   especially as they are implicated in disrupting biofilm formation (27, 76, 77). Metal toxicity

568   could also be harnessed in the presence of chelants that selectively restrict availability of

569   iron, manganese and zinc to mimic the killing achieved in phagocytic vesicles (78).

570   Modelling bacterial uptake of metals will assist in identifying the specificity of molecules for

571   manipulating metal acquisition. Affinity ratios can identify which chelants preferentially

572   interfere with which metals for uptake as exemplified by $\log(K_{Fe(III)}:K_{Mn(II)})$ values for the

573   iron-selective chelator HBED (24.9) which exceeds values estimated for Fe(III) versus

574   Mn(II) uptake (22.1), and exceeds values for DTPA, GLDA, EDTA and MGDA ($\leq$14.4)

575   which preferentially target manganese.

576   The results from this study show that in most cases it is challenging to predict,

577   especially from available empirical metal ion affinity data, which combinations are likely to

578   be most effective (79). However, we now have a much clearer understanding of the metals

579   affected and indications that the cellular sites of metal sequestration may differ between

580   them. Significantly, a large number of synergistic antibacterial chelant combinations have

581   been identified that could be incorporated into products where their preservation properties

582 are desirable. New formulations can be manufactured that reduce the quantities of

583 chelants required and integrate biodegradable alternatives (e.g. GLDA/MGDA) with major

584 benefits for sustainability and environmental compatibility. Further work is needed to

585 rationalize our predictive capabilities with chelating agents and define precisely: (i) the

586 localization of chelants within cells, (ii) robust metal ion affinities for chelators to multiple

587 metal ions *in vitro*, (iii) how these affinities compare with the availabilities (buffered

588 concentrations / free energies) of the elements at their respective locations (80), and (iv)

589 whether bacterial species with different cell wall structures and metal uptake strategies

590 exhibit similar cellular responses.

591 **MATERIALS AND METHODS**

592 **Bacterial growth inhibition by chelants.** Chelating agents were obtained commercially

593 and are listed in Table S5. Most chelants were soluble in water, but CHA, HBED and PO

594 were resuspended in dimethyl sulphoxide (DMSO) and TPEN in ethanol. Appropriate

595 vehicle controls were performed in parallel for all growth experiments involving these

596 chelants. *E. coli* K-12 BW25113 (*rrnB3 ΔlacZ4787 hsdR514 Δ(araBAD)567 Δ(rhaBAD)568*

597 *rph-1*) and deletion-insertion derivatives from the Keio collection (38) were used in this

598 study. For microdilution MIC assays, *E. coli* cultures were grown in LB media (Lennox,

599 Sigma Aldrich) or MOPS-minimal media (Teknova Inc) in an orbital shaker (Stuart) at 37°C

600 to an OD_{650nm} of 0.07, equivalent to a 0.5 MacFarland standard (240 μM $BaCl_2$ in 0.18 M

601 H_2SO_4 aq.) and diluted 10-fold in LB broth for use as an inoculum (65). The diluted culture

602 (50 μl, 5 x 10^6 CFU/ml) was then transferred into a 96-well, round-bottomed microtitre

603 plate (Sarstedt). Chelants from stock samples, prepared in water, DMSO or ethanol, were

604 diluted to yield a 2-fold series in LB broth and 50 μl mixed with the diluted inoculum. Plates

605 were incubated at 37°C with shaking at 130 rpm for 16 h and absorbance (A_{600nm} or

606 A_{650nm}) monitored on a Spectrostar Nano plate reader. MICs were defined as the minimum

607 concentration of chelant needed to inhibit growth by >90% relative to controls.

24

608   Checkerboard assays were performed to assess the effect of chelants in combination.

609   Stock solutions and inoculum were prepared as for MIC experiments. One chelator was

610   applied in decreasing concentrations horizontally across the 96-well microtitre plate, while

611   the second chelator was added in decreasing concentrations vertically to create the

612   checkerboard (Supplemental Material Data File S1). A Fractional Inhibitory Concentration

613   index (FICI) was defined as the minimum concentration of chelant needed to inhibit growth

614   by >90% individually and in combination and FIC index values were interpreted as

615   synergistic (≤0.5), indifferent (>0.5-4.0) or antagonistic (>4) based on published methods

616   (66, 67) and according to the formula shown in Figure 4.

617   **Isolation of piroctone from piroctone olamine.** PO was dissolved in the minimum

618   amount of methanol prior to the addition of 1M HCl (until pH 1 was reached). The mixture

619   was then transferred to a separating funnel, diluted with either DCM or chloroform and the

620   organic layer collected, dried over $MgSO_4$ and the solvent removed *in vacuo*. Drying the

621   resulting solid to constant weight using a high vacuum line afforded piroctone as an off-

622   white powder. ^{1}H NMR (400 MHz, DMSO) δ 6.19 (d, 1H), 5.93 (d, 1H), 2.59 (dd, 1H), 2.38

623   (dd, 1H), 2.10 (s, 3H), 2.08 (d, 3H), 2.03 – 1.91 (m, 1H), 1.26 (dd, 1H), 1.08 (dd, 1H), 0.88

624   (d, 3H), 0.82 (s, 9H).

625   **β-galactosidase assays to monitor *mntH-lacZ* promoter activity.** SIP879 (*mntH*::

626   Mud1(Ap, *lac*) *aroB*) and SIP943 (*mntH*::Mud1(Ap, *lac*) *aroB mntR*) are *E. coli* K-12

627   derivatives of MC4100 (*araD139* Δ(*lacIZYA-argF*)*U169 rpsL150 relA1 flhD5301 deoC1*

628   *fruA25 rbsR22*) (59) and were kindly provided by Laura Runyen-Janecky. Promoter activity

629   assays were performed as described previously (81). Briefly, bacteria were cultivated in LB

630   broth in sterile cuvettes (1 ml) in the presence or absence of chelant or $MnCl_2$ to an A_{600nm}

631   of 0.5. 80 μl of culture was transferred to a 96-well microtitre plate followed by addition of

632   120 μl master mix (60 mM Na_2HPO_4, 40 mM NaH_2PO_4, 10 mM KCl, 1 mM $MgSO_4$, 36 mM

633   β-mercaptoethanol, 166 μl/ml T7 lysozyme, 1.1 mg/ml ONPG and 6.7% PopCulture

25

634   Reagent obtained from Merck Millipore). This was then transferred to a SPECTROstar

635   Nano absorbance plate reader (BMG LABTECH) set to 30°C with shaking at 400 rpm, with

636   absorbance readings taken at 420 and 550 nm every minute for 1 hour. Miller Units were

637   calculated using the following equation 1000 x $[(A_{420nm} - 1.75 \times OD_{550nm})] / (T \times V \times A_{600nm})$

638   where T = time in minutes, and V = volume in ml (0.2).

639   **Keio collection screen.** The duplicate set of 3985 Keio library mutants, 7970 strains in

640   total (38), were grown in 200 µl LB media without antibiotic supplementation at 37°C with

641   27 or 34 µM PO in 96-well microtitre plates for 16 h. A Versette Automated Liquid Handler

642   (ThermoFisher) was used to dispense media and treatments, and inoculate the library.

643   Percentage growth was determined by comparison of A_{600nm}, using a SpectraMax plate

644   reader (Molecular Devices), with untreated controls for each strain.

645   **Determination of cellular metal content.** Different concentrations of chelant were added

646   to 50 ml LB broth in 250 ml acid washed conical flasks prior to inoculation with 1 x 10^7 *E.*

647   *coli* BW25113 cells. Cultures were grown at 37°C in an orbital shaker at 130 rpm with the

648   aim of inhibiting growth by 10-15% during mid-log phase (~0.3-0.4 A_{650nm}, typically 3-4

649   hours of growth). Cell numbers were recorded using a Casy Model TT Cell Counter prior to

650   harvesting. Cells were pelleted by centrifugation (19,000 g, 25 min) and resuspended in 50

651   ml wash buffer (0.5 M sorbitol, 10 mM HEPES pH7.8) and centrifuged once again at

652   19000 g for 25 min. The cell pellet was then digested in 5 ml, 65% nitric acid (Suprapur®,

653   Sigma Aldrich) for a minimum of 16 h. These pellet digests were diluted with 2% nitric acid

654   and 5.89 x 10^{-4} µM silver standard for ICP (Sigma Aldrich) in a 1:8:1 ratio. Calibration

655   samples were made using known quantities of metals in nitric acid (ICP multi-element

656   standards, CertiPUR®, Sigma Aldrich & Merck) diluted in matrix-matched solution.

657   Dilutions and a calibration curve were analysed using inductively coupled plasma mass

658   spectrometry (ICP-MS, Thermo XSERIES 2). Instrument control, analysis and

659   quantification was obtained using software interface PlasmaLab (Thermo Scientific) and

26

660 further analysis was conducted in Microsoft Excel. Mean and standard deviation values

661 were determined from triplicate biological analyses.

ACKNOWLEDGMENTS

CONFLICT OF INTEREST STATEMENT

680

References

681 **References**

682 1. Hood MI, Skaar EP. 2012. Nutritional immunity: transition metals at the pathogen-host
683   interface. Nat Rev Microbiol 10:525-537.

684 2. Palmer LD, Skaar EP. 2016. Transition metals and virulence in bacteria. Ann Rev
685   Genet 50:67-91.

686 3. Chandrangsu P, Rensing C, Helmann JD. 2017. Metal homeostasis and resistance in
687   bacteria. Nat Rev Microbiol 15:338-350.

688 4. Schmidt CK, Fleig M, Sacher F, Brauch HJ. 2004. Occurrence of
689   aminopolycarboxylates in the aquatic environment of Germany. Environ Pollut
690   131:107-124.

691 5. Knepper TP. 2003. Synthetic chelating agents and compounds exhibiting complexing
692   properties in the aquatic environment. Trends Analyt Chem 22:708–724.

693 6. Nowack B, VanBriesen JM. 2005. Chelating agents in the environment., p 1-18. *In*
694   Nowack B, VanBriesen JM (ed), Biogeochemistry of chelating agents. American
695   Chemical Society, Washington, DC.

696 7. Brown MR, Richards RM. 1965. Effect of ethylenediamine tetraacetate on the
697   resistance of *Pseudomonas aeruginosa* to antibacterial agents. Nature 207:1391-
698   1393.

699 8. Lambert RJ, Hanlon GW, Denyer SP. 2004. The synergistic effect of
700   EDTA/antimicrobial combinations on *Pseudomonas aeruginosa*. J Appl Microbiol
701   96:244-253.

702 9. Vaara M. 1992. Agents that increase the permeability of the outer membrane.
703   Microbiol Rev 56:395-411.

704 10. Hart JR. 1984. Chelating agents as preservative potentiators., p 323-337. *In* Kabara JJ
705   (ed), Cosmetic and drug preservation: principles and practice. Marcel Dekker, New
706   York.

707 11. Schindler M, Osborn MJ. 1979. Interaction of divalent cations and polymyxin B with
708   lipopolysaccharide. Biochemistry 18:4425-4430.

709 12. Marvin HJ, ter Beest MB, Witholt B. 1989. Release of outer membrane fragments from
710   wild-type *Escherichia coli* and from several *E. coli* lipopolysaccharide mutants by
711   EDTA and heat shock treatments. J Bacteriol 171:5262-5267.

712 13. Pelletier C, Bourlioux P, van Heijenoort J. 1994. Effects of sub-minimal inhibitory
713   concentrations of EDTA on growth of *Escherichia coli* and the release of
714   lipopolysaccharide. FEMS Microbiol Lett 117:203-206.

715 14. Clifton LA, Skoda MW, Le Brun AP, Ciesielski F, Kuzmenko I, Holt SA, Lakey JH.
716   2015. Effect of divalent cation removal on the structure of gram-negative bacterial
717   outer membrane models. Langmuir 31:404-412.

718 15. Voss JG. 1967. Effects of organic cations on the gram-negative cell wall and their
719   bactericidal activity with ethylenediaminetetra-acetate and surface active agents. J
720   Gen Microbiol 48:391-400.

721 16. Leive L. 1965. Release of lipopolysaccharide by EDTA treatment of *E. coli*. Biochem
722   Biophys Res Commun 21:290-296.

723 17. Leive L. 1974. The barrier function of the gram-negative envelope. Ann N Y Acad Sci
724   235:109-129.

725 18. Scudamore RA, Beveridge TJ, Goldner M. 1979. Outer-membrane penetration barriers
726   as components of intrinsic resistance to beta-lactam and other antibiotics in
727   *Escherichia coli* K-12. Antimicrob Agents Chemother 15:182-189.

728 19. Spicer AB, Spooner DF. 1974. The inhibition of growth of *Escherichia coli* spheroplasts
729   by antibacterial agents. J Gen Microbiol 80:37-50.

730   20. Alakomi HL, Skytta E, Saarela M, Mattila-Sandholm T, Latva-Kala K, Helander IM.
731   2000. Lactic acid permeabilizes gram-negative bacteria by disrupting the outer
732   membrane. Appl Environ Microbiol 66:2001-2005.
733   21. Alakomi HL, Saarela M, Helander IM. 2003. Effect of EDTA on *Salmonella enterica*
734   serovar Typhimurium involves a component not assignable to lipopolysaccharide
735   release. Microbiology 149:2015-2021.
736   22. Haque H, Russell AD. 1974. Effect of chelating agents on the susceptibility of some
737   strains of gram-negative bacteria to some antibacterial agents. Antimicrob Agents
738   Chemother 6:200-206.
739   23. Haque H, Russell AD. 1974. Effect of ethylenediaminetetraacetic acid and related
740   chelating agents on whole cells of gram-negative bacteria. Antimicrob Agents
741   Chemother 5:447-452.
742   24. Weiser R, Wimpenny J, Asscher AW. 1969. Synergistic effect of edetic-acid/antibiotic
743   combinations on *Pseudomonas aeruginosa*. Lancet 2:619-620.
744   25. Angus BL, Carey AM, Caron DA, Kropinski AM, Hancock RE. 1982. Outer membrane
745   permeability in *Pseudomonas aeruginosa*: comparison of a wild-type with an antibiotic-
746   supersusceptible mutant. Antimicrob Agents Chemother 21:299-309.
747   26. Amro NA, Kotra LP, Wadu-Mesthrige K, Bulychev A, Mobashery S, Liu G-Y. 2000.
748   High-resolution atomic force microscopy studies of the *Escherichia coli* outer
749   membrane: structural basis for permeability. Langmuir 16:2789-2796.
750   27. Alakomi HL, Paananen A, Suihko ML, Helander IM, Saarela M. 2006. Weakening
751   effect of cell permeabilizers on gram-negative bacteria causing biodeterioration. Appl
752   Environ Microbiol 72:4695-4703.
753   28. Prachayasittikul V, Isarankura-Na-Ayudhya C, Tantimongcolwat T, Nantasenamat C,
754   Galla HJ. 2007. EDTA-induced membrane fluidization and destabilization: biophysical
755   studies on artificial lipid membranes. Acta Biochim Biophys Sin (Shanghai) 39:901-
756   913.
757   29. Pinto IS, Neto IF, Soares HM. 2014. Biodegradable chelating agents for industrial,
758   domestic, and agricultural applications - a review. Environ Sci Pollut Res Int 21:11893-
759   11906.
760   30. Hancock RD. 1992. Chelate ring size and metal ion selection: the basis of selectivity
761   for metal ions in open-chain ligands and macrocycles. J Chem Educ 69:615-621.
762   31. Hancock RD, Martell AE. 1989. Ligand design for selective complexation of metal ions
763   in aqueous solution. Chem Rev 89:1875-1914.
764   32. Pettit LD. 2009. The IUPAC stability constants database. Chemistry International -
765   Newsmagazine for IUPAC 28:14-15, https://doi.org/10.1515/ci.2006.28.5.14.
766   33. L'Eplattenier F, Murase A, Martell E. 1967. New multidentate ligands. VI. Chelating
767   tendencies of N,N′-Di(2-hydroxybenzyl)ethylenediamine-N,N′-diacetic acid. J Am
768   Chem Soc 89:837-843.
769   34. Sanchez P, Galvez N, Colacio E, Minones E, Dominguez-Vera JM. 2005. Catechol
770   releases iron(III) from ferritin by direct chelation without iron(II) production. Dalton
771   Trans doi:10.1039/b416669h:811-813.
772   35. Sidarovich V, Adami V, Gatto P, Greco V, Tebaldi T, Tonini GP, Quattrone A. 2015.
773   Translational downregulation of HSP90 expression by iron chelators in neuroblastoma
774   cells. Mol Pharmacol 87:513-524.
775   36. Haase H, Hebel S, Engelhardt G, Rink L. 2013. Application of Zinpyr-1 for the
776   investigation of zinc signals in *Escherichia coli*. Biometals 26:167-177.
777   37. Rapisarda VA, Volentini SI, Farias RN, Massa EM. 2002. Quenching of bathocuproine
778   disulfonate fluorescence by Cu(I) as a basis for copper quantification. Anal Biochem
779   307:105-109.

29

780 38. Baba T, Ara T, Hasegawa M, Takai Y, Okumura Y, Baba M, Datsenko KA, Tomita M,
781   Wanner BL, Mori H. 2006. Construction of *Escherichia coli* K-12 in-frame, single-gene
782   knockout mutants: the Keio collection. Mol Syst Biol 2:2006 0008.

783 39. Sezonov G, Joseleau-Petit D, D'Ari R. 2007. *Escherichia coli* physiology in Luria-
784   Bertani broth. J Bacteriol 189:8746-8749.

785 40. Wiegand I, Hilpert K, Hancock RE. 2008. Agar and broth dilution methods to determine
786   the minimal inhibitory concentration (MIC) of antimicrobial substances. Nat Protoc
787   3:163-175.

788 41. Neidhardt FC, Bloch PL, Smith DF. 1974. Culture medium for enterobacteria. J
789   Bacteriol 119:736-747.

790 42. Outten CE, O'Halloran TV. 2001. Femtomolar sensitivity of metalloregulatory proteins
791   controlling zinc homeostasis. Science 292:2488-2492.

792 43. Outten CE. 2001. Mechanistic studies of metalloregulatory proteins controlling metal
793   ion homeostasis in *Escherichia coli*. Doctoral dissertation. Northwestern University.

794 44. Graham AI, Hunt S, Stokes SL, Bramall N, Bunch J, Cox AG, McLeod CW, Poole RK.
795   2009. Severe zinc depletion of *Escherichia coli*: roles for high affinity zinc binding by
796   ZinT, zinc transport and zinc-independent proteins. J Biol Chem 284:18377-18389.

797 45. Imlay JA. 2014. The mismetallation of enzymes during oxidative stress. J Biol Chem
798   289:28121-28128.

799 46. Sargent F. 2016. The model [NiFe]-hydrogenases of *Escherichia coli*. Adv Microb
800   Physiol 68:433-507.

801 47. Miller AF. 2012. Superoxide dismutases: ancient enzymes and new insights. FEBS
802   Lett 586:585-595.

803 48. Andrews SC. 2011. Making DNA without iron - induction of a manganese-dependent
804   ribonucleotide reductase in response to iron starvation. Mol Microbiol 80:286-289.

805 49. Breckau D, Mahlitz E, Sauerwald A, Layer G, Jahn D. 2003. Oxygen-dependent
806   coproporphyrinogen III oxidase (HemF) from *Escherichia coli* is stimulated by
807   manganese. J Biol Chem 278:46625-46631.

808 50. Cotruvo JA, Jr., Stubbe J. 2012. Metallation and mismetallation of iron and
809   manganese proteins *in vitro* and *in vivo*: the class I ribonucleotide reductases as a
810   case study. Metallomics 4:1020-1036.

811 51. Lisher JP, Giedroc DP. 2013. Manganese acquisition and homeostasis at the host-
812   pathogen interface. Front Cell Infect Microbiol 3:91.

813 52. Anjem A, Varghese S, Imlay JA. 2009. Manganese import is a key element of the
814   OxyR response to hydrogen peroxide in *Escherichia coli*. Mol Microbiol 72:844-858.

815 53. Brown MR, Melling J. 1969. Role of divalent cations in the action of polymyxin B and
816   EDTA on *Pseudomonas aeruginosa*. J Gen Microbiol 59:263-274.

817 54. Hassan HM, Schrum LW. 1994. Roles of manganese and iron in the regulation of the
818   biosynthesis of manganese-superoxide dismutase in *Escherichia coli*. FEMS Microbiol
819   Rev 14:315-323.

820 55. Juttukonda LJ, Skaar EP. 2015. Manganese homeostasis and utilization in pathogenic
821   bacteria. Mol Microbiol 97:216-228.

822 56. Seo SW, Kim D, Latif H, O'Brien EJ, Szubin R, Palsson BO. 2014. Deciphering Fur
823   transcriptional regulatory network highlights its complex role beyond iron metabolism
824   in *Escherichia coli*. Nat Commun 5:4910.

825 57. Escolar L, Perez-Martin J, de Lorenzo V. 1999. Opening the iron box: transcriptional
826   metalloregulation by the Fur protein. J Bacteriol 181:6223-6229.

827 58. Sarvan S, Butcher J, Stintzi A, Couture JF. 2018. Variation on a theme: investigating
828   the structural repertoires used by ferric uptake regulators to control gene expression.
829   Biometals 31:681-704.
830 59. Patzer SI, Hantke K. 2001. Dual repression by Fe^{2+}-Fur and Mn^{2+}-MntR of the *mntH*
831   gene, encoding an NRAMP-like Mn^{2+} transporter in *Escherichia coli.* J Bacteriol
832   183:4806-4813.
833 60. Niederhoffer EC, Naranjo CM, Bradley KL, Fee JA. 1990. Control of *Escherichia coli*
834   superoxide dismutase (*sodA and sodB*) genes by the ferric uptake regulation (*fur*)
835   locus. J Bacteriol 172:1930-1938.
836 61. Dubrac S, Touati D. 2000. Fur positive regulation of iron superoxide dismutase in
837   *Escherichia coli*: functional analysis of the *sodB* promoter. J Bacteriol 182:3802-3808.
838 62. Kehres DG, Janakiraman A, Slauch JM, Maguire ME. 2002. Regulation of *Salmonella*
839   *enterica* serovar Typhimurium *mntH* transcription by H_2O_2, Fe^{2+}, and Mn^{2+}. J Bacteriol
840   184:3151-3158.
841 63. Sigdel TK, Easton JA, Crowder MW. 2006. Transcriptional response of *Escherichia*
842   *coli* to TPEN. J Bacteriol 188:6709-6713.
843 64. Mikhaylina A, Ksibe AZ, Scanlan DJ, Blindauer CA. 2018. Bacterial zinc uptake
844   regulator proteins and their regulons. Biochem Soc Trans 46:983-1001.
845 65. Andrews JM. 2001. Determination of minimum inhibitory concentrations. J Antimicrob
846   Chemother 48 Suppl 1:5-16.
847 66. Leber A. 2016. Synergism testing: broth microdilution checkerboard and broth
848   macrodilution methods. *In* Garcia LS (ed), Clinical Microbiology Procedures
849   Handbook, 4th ed doi:10.1128/9781555818814.ch5.16. ASM Press, Washington, DC.
850 67. Bonapace CR, Bosso JA, Friedrich LV, White RL. 2002. Comparison of methods of
851   interpretation of checkerboard synergy testing. Diagn Microbiol Infect Dis 44:363-366.
852 68. Bijlsma J, de Bruijn WJC, Hageman JA, Goos P, Velikov KP, Vincken J-P. 2020.
853   Revealing the main factors and two-way interactions contributing to food discolouration
854   caused by iron-catechol complexation. Sci Rep 10:8288.
855 69. Nichols RJ, Sen S, Choo YJ, Beltrao P, Zietek M, Chaba R, Lee S, Kazmierczak KM,
856   Lee KJ, Wong A, Shales M, Lovett S, Winkler ME, Krogan NJ, Typas A, Gross CA.
857   2011. Phenotypic landscape of a bacterial cell. Cell 144:143-156.
858 70. Smith DR, Chapman MR. 2010. Economical evolution: microbes reduce the synthetic
859   cost of extracellular proteins. mBio 1:e00131-10.
860 71. Raymond KN, Dertz EA, Kim SS. 2003. Enterobactin: an archetype for microbial iron
861   transport. Proc Natl Acad Sci USA 100:3584-3588.
862 72. Lonergan ZR, Skaar EP. 2019. Nutrient zinc at the host-pathogen interface. Trends
863   Biochem Sci 44:1041-1056.
864 73. Miethke M. 2013. Molecular strategies of microbial iron assimilation: from high-affinity
865   complexes to cofactor assembly systems. Metallomics 5:15-28.
866 74. Kern T, Giffard M, Hediger S, Amoroso A, Giustini C, Bui NK, Joris B, Bougault C,
867   Vollmer W, Simorre JP. 2010. Dynamics characterization of fully hydrated bacterial cell
868   walls by solid-state NMR: evidence for cooperative binding of metal ions. J Am Chem
869   Soc 132:10911-9.
870 75. Silva AM, Kong X, Parkin MC, Cammack R, Hider RC. 2009. Iron(III) citrate speciation
871   in aqueous solution. Dalton Trans doi:10.1039/b910970f:8616-8625.
872 76. Banin E, Brady KM, Greenberg EP. 2006. Chelator-induced dispersal and killing of
873   *Pseudomonas aeruginosa* cells in a biofilm. Appl Environ Microbiol 72:2064-2069.
874 77. Finnegan S, Percival SL. 2015. EDTA: an antimicrobial and antibiofilm agent for use in
875   wound care. Adv Wound Care (New Rochelle) 4:415-421.

31

876   78. Lemire JA, Harrison JJ, Turner RJ. 2013. Antimicrobial activity of metals: mechanisms,
877   molecular targets and applications. Nat Rev Microbiol 11:371-384.
878   79. Mulla RS, Beecroft MS, Pal R, Aguilar JA, Pitarch-Jarque J, Garcia-Espana E, Lurie-
879   Luke E, Sharples GJ, Gareth Williams JA. 2018. On the antibacterial activity of
880   azacarboxylate ligands: lowered metal ion affinities for bis-amide derivatives of EDTA
881   do not mean reduced activity. Chemistry 24:7137-7148.
882   80. Osman D, Martini MA, Foster AW, Chen J, Scott AJP, Morton RJ, Steed JW, Lurie-
883   Luke E, Huggins TG, Lawrence AD, Deery E, Warren MJ, Chivers PT, Robinson NJ.
884   2019. Bacterial sensors define intracellular free energies for correct enzyme
885   metalation. Nat Chem Biol 15:241-249.
886   81. Schaefer J, Jovanovic G, Kotta-Loizou I, Buck M. 2016. Single-step method for β-
887   galactosidase assays in *Escherichia coli* using a 96-well microplate reader. Anal
888   Biochem 503:56-57.
889   82. Garenaux A, Caza M, Dozois CM. 2011. The ins and outs of siderophore mediated
890   iron uptake by extra-intestinal pathogenic *Escherichia coli*. Vet Microbiol 153:89-98.
891   83. Brickman TJ, McIntosh MA. 1992. Overexpression and purification of ferric
892   enterobactin esterase from *Escherichia coli*: demonstration of enzymatic hydrolysis of
893   enterobactin and its iron complex. J Biol Chem 267:12350-12355.
894   84. Patzer SI, Hantke K. 1998. The ZnuABC high-affinity zinc uptake system and its
895   regulator Zur in *Escherichia coli*. Mol Microbiol 28:1199-1210.
896   85. Harris WR, Carrano CJ, Raymond KN. 1979. Spectrophotometric determination of the
897   proton-dependent stability constant of ferric enterobactin. J Am Chem Soc 101:2213-
898   2214.
899   86. Loomis LD, Raymond KN. 1991. Solution equilibria of enterobactin and metal-
900   enterobactin complexes. Inorg Chem 30:906-911.
901   87. Martell AE, Smith RM. 1974. Critical stability constants. Springer, New. York, London.
902   88. Gribenko A, Mosyak L, Ghosh S, Parris K, Svenson K, Moran J, Chu L, Li S, Liu T,
903   Woods VL, Jr., Jansen KU, Green BA, Anderson AS, Matsuka YV. 2013. Three-
904   dimensional structure and biophysical characterization of *Staphylococcus aureus* cell
905   surface antigen-manganese transporter MntC. J Mol Biol 425:3429-3445.
906

907 **Figure legends**

908 **FIG 1** Structure of chelants selected for analysis. BCS (bathocuproine disulphonic acid),

909 CAT (catechol), CHA (caprylhydroxamic acid), DTPA (diethylenetriaminepentaacetic acid),

910 DTPMP (diethylenetriaminepentamethylene phosphonic acid), EDTA

911 (ethylenediaminetetraacetic acid), GLDA (glutamic acid-N,N-diacetic acid), HBED (N,N-bis

912 (2-hydroxybenzyl) ethylenediamine-N,N-diacetic acid), MGDA (methylglycinediacetic acid),

913 PO (piroctone olamine) and TPEN (N,N,N',N'-tetrakis (2-pyridylmethyl) ethylenediamine).

914 The most biodegradable isomer of GLDA (L-GLDA) is shown.

915 **FIG 2** Effect of chelants on *E. coli* growth in LB. Bacteria were cultivated in LB (Lennox)

916 media and mixed with appropriate 2-fold dilutions of each chelant and incubated with

917 shaking for 16 h at 37°C. Results are the mean and standard deviation of an independent

918 experiment performed in triplicate; a further two independent experiments performed in

919 triplicate yielded similar results. MICs in mM are based on >90% growth inhibition, where

920 achieved, as indicated at the bottom right of the figure; they were determined for LB and

921 MOPS-minimal media from 3 and 4 biological replicates, respectively.

922 **FIG 3** Effect of chelants on the metal composition of *E. coli*. Chelants are grouped

923 according to the similarity in their effects on cellular metal concentration (i-iv) as described

924 in the text. Selected results correspond to growth inhibition of 10-15% and the amount of

925 each metal determined in atoms per cell using ICP-MS. BW25113 cells were grown in 50

926 ml of LB pH7 to log-phase in a shaking incubator (125 rpm) at 37°C. Data are the mean

927 and standard deviation of 3 independent biological replicates (one-way ANOVA comparing

928 each chelant concentration with the untreated control in each case, $**P < 0.01$, $***P <$

929 0.001, $****P < 0.0001$). Concentrations of each chelant are indicated below each set of

930 graphs. The original data were determined over a range of chelant concentrations in most

931 cases and a full summary is provided in Table S2.

33

932 **FIG 4** Chelant combinations analysed by the checkerboard assay. Examples of (A)

933 synergistic, (B) indifferent and (C) antagonistic pairings, for CHA/DTPMP, CAT/PO and

934 BCS/TPEN, respectively, are shown. (D) FIC index values are shown for two independent

935 experiments performed in triplicate for each chelant combination. The assay allows the

936 calculation of an MIC for each chelant and hence the FIC, which provides a measure of

937 the effect of the chelants in combination as synergistic, indifferent or antagonistic. FIC

938 index values were calculated based on the lowest concentration of each chelant in

939 combination divided by the MIC for that chelant according to the formula shown. Two-fold

940 dilutions (as in an MIC) of chelants were performed in LB broth with *E. coli* BW25113 at

941 37°C with shaking at 37°C for 16 h. Additional controls for low levels of DMSO, ethanol or

942 water were included where relevant.

943 **FIG 5** Effect of selected chelant combinations on total cellular metal content. (A) 14 µM PO

944 with addition of 2, 4, 6, 7, 7.5, 8, 8.5, 9.5 and 10 µM DTPA. (B) 10 µM DTPMP with

945 addition of 12, 13, 14, 15 and 16 µM PO. (C) 15 µM PO with addition of 1.25, 2.5, 3.75, 5,

946 6.25, 7.5, 8.75 and 10 µM DTPMP. Concentrations of each chelant used are indicated

947 below each set of graphs. Results correspond to growth inhibition of 10-30% (grey bars in

948 the topmost graphs) and the amount of each metal determined in atoms per cell using

949 ICP-MS. BW25113 cells were grown in 50 ml of LB to log-phase in a shaking incubator at

950 37°C. Data are the mean and standard deviation of 3 independent biological replicates

951 (one-way ANOVA comparing each chelant concentration with the untreated control in each

952 case or between single chelant treatment with addition of a second chelant as indicated,

953 *$P < 0.05$, **$P < 0.01$, ***$P < 0.001$). Although some experiments were subject to

954 variability, there were consistent trends with Fe, Mn and Zn levels in each of the three

955 independent experiments in some cases; for these metal ions, the data points are

956 highlighted as differently-coloured symbols to show the pattern of each of the three

957 replicates.

34

958   **FIG 6** Effect of PO on the growth of *E. coli* mutants from the Keio collection. (A) The

959   duplicate set of 3985 Keio library mutants (38), 7970 strains in total, were grown in LB

960   media at 37°C with 27 or 34 µM PO for 16 h. Percentage growth was compared to

961   untreated controls for each strain and the top 50 slowest growing mutants are shown (see

962   Supplemental Material Data File S2). Where two percentages under each condition are

963   shown, these correspond to the presence of both duplicates from the Keio collection in the

964   top 200 slowest growing mutants identified in the screen. Each mutant is colour-coded

965   based on the functional grouping assigned for each gene with the key shown in (C). (B)

966   The 50 slowest growing mutants identified from the Keio phenotypic screen using EDTA

967   (69) is shown to facilitate comparisons with PO. The more negative pixel score values

968   correspond to the poorest colony growth on agar plates supplemented with 0.5 mM EDTA.

969   (C) The ferric enterobactin synthesis, export and import system of *E. coli*. Key proteins

970   involved in each part of the iron uptake system are colour-coded according to their roles

971   (71, 73). AroA-M proteins are involved in the biosynthesis of chorismate that is converted

972   by EntABC to 2,3-dihydroxybenzoic acid (DHB). EntDEF catalyse DHB and L-serine

973   linkage and ultimate assembly into enterobactin (71), which is exported to the extracellular

974   environment by EntS and TolC (82). The ferric-enterobactin complex is recovered by

975   association with the outer membrane receptor FepA. The TonB/ExbBD complex provides

976   energy from the proton motive force to mediate release of the Fe(III)-enterobactin complex

977   from FepA, facilitated by FepB, and delivery to the FepCDG ABC-family, ATP-dependent

978   inner membrane permease (71). Upon reaching the cytosol, Fe(III) is released from the

979   siderophore by the Fes esterase (83). Another ABC-family transporter, ZnuABC,

980   transports Zn(II) across the inner membrane (72, 84). Outer and inner membranes are

981   depicted as lipid bilayers with the lower portion of the diagram shaded in blue to represent

982   the cytosol. Where substantially-reduced growth is associated with mutation of key ferric-

35

983   siderophore synthesis and transport components, these are indicated with cyan and blue

984   (PO) and green (EDTA) symbols.

985   **FIG 7** Selected *E. coli* mutant sensitivity to (A) PO, (B) DTPMP and (C) EDTA. Bacteria

986   were incubated with a two-fold serial dilution of each chelant in 100 µl of LB media and

987   incubated with shaking for 16 h at 37°C. Absorbance at 600 nm was recorded and the

988   percentage growth calculated for each strain. Data represent the mean and standard

989   deviation of an independent experiment performed in triplicate. A second biological repeat

990   was performed and a similar pattern of susceptibility was observed.

991   **FIG 8** Relative Fe(III) and Mn(II) affinities of chelants which primarily restrict either Fe(III)

992   (in red) or Mn(II) (in blue) accumulation in cells (judged by % reduction of metal content in

993   chelant-treated cells compared to untreated controls). The relative metal affinities of

994   selected components of uptake systems for iron or manganese at the cell surface are

995   shown by the red dotted lines: The association constants of Fe(III)-enterobactin and

996   Fe(III)-citrate at pH 7.0 were calculated using reported pH-independent affinities of ligands

997   and pK_a values of coordinating atoms (85-87); the Mn(II) affinity of *S. aureus* MntC (solute

998   binding protein) was used in the absence of a known affinity of the *E. coli* manganese

999   transporter MntH (88); a 'pseudo-affinity' of the Fe(III)(citrate)$_2$ complex was derived from

1000   the calculated pFe^{3+} at pH 7.4 when [Fe(III)]$_{tot}$ = 1 µM and [citrate]$_{tot}$ = 100 µM (75).

36

BCS

CAT

CHA

DTPA

DTPMP

EDTA

GLDA

HBED

MGDA

PO

TPEN

MIC (mM)	LB	MOPS
BCS	>100	>100
CAT	15	2.5
CHA	1.25	2.5
DTPA	1.25	0.5
DTPMP	4.4	5
EDTA	25	2.5
GLDA	31.25	25
HBED	5	10
MGDA	31.25	25
PO	0.075	0.25
TPEN	0.4	0.2

A   Synergistic

B   Indifferent

C   Antagonistic
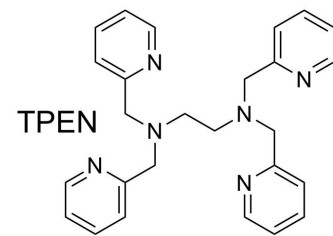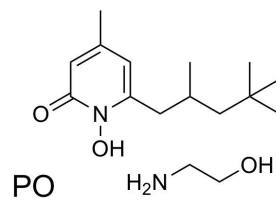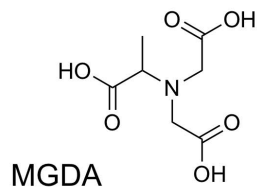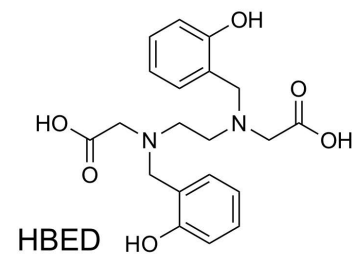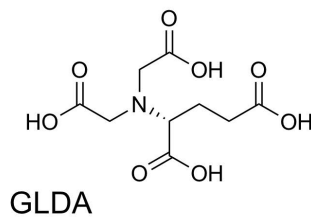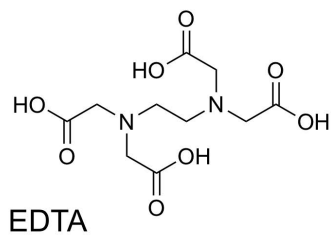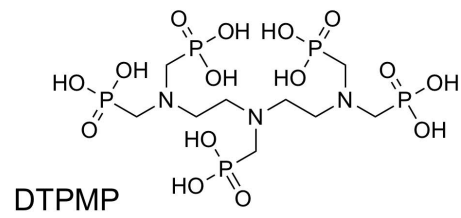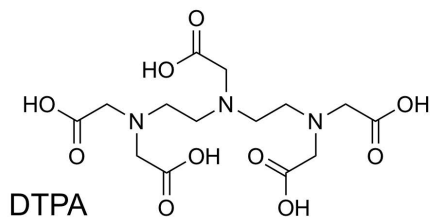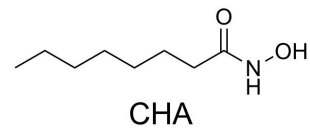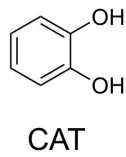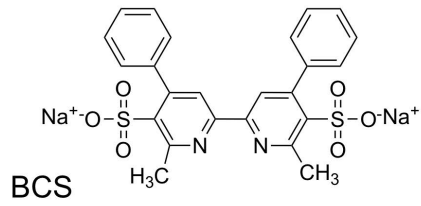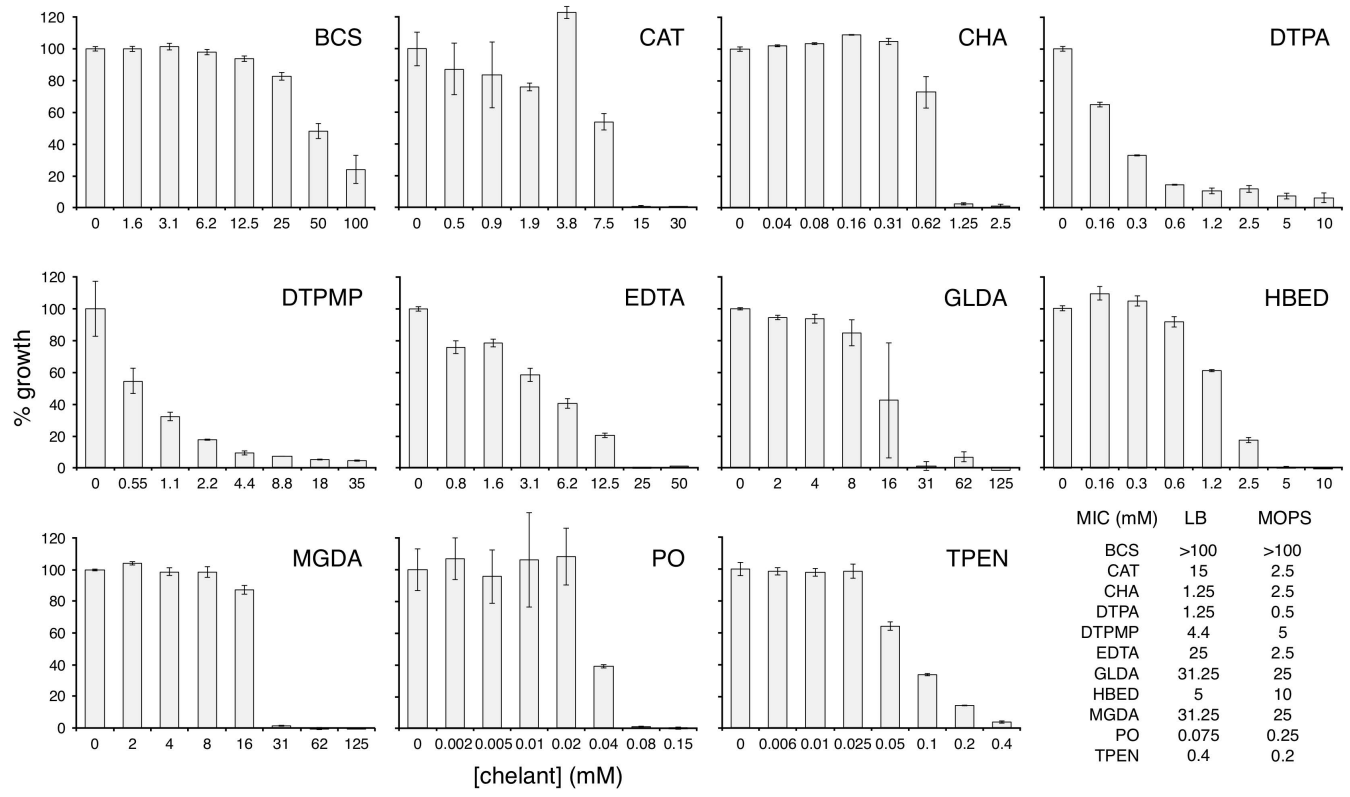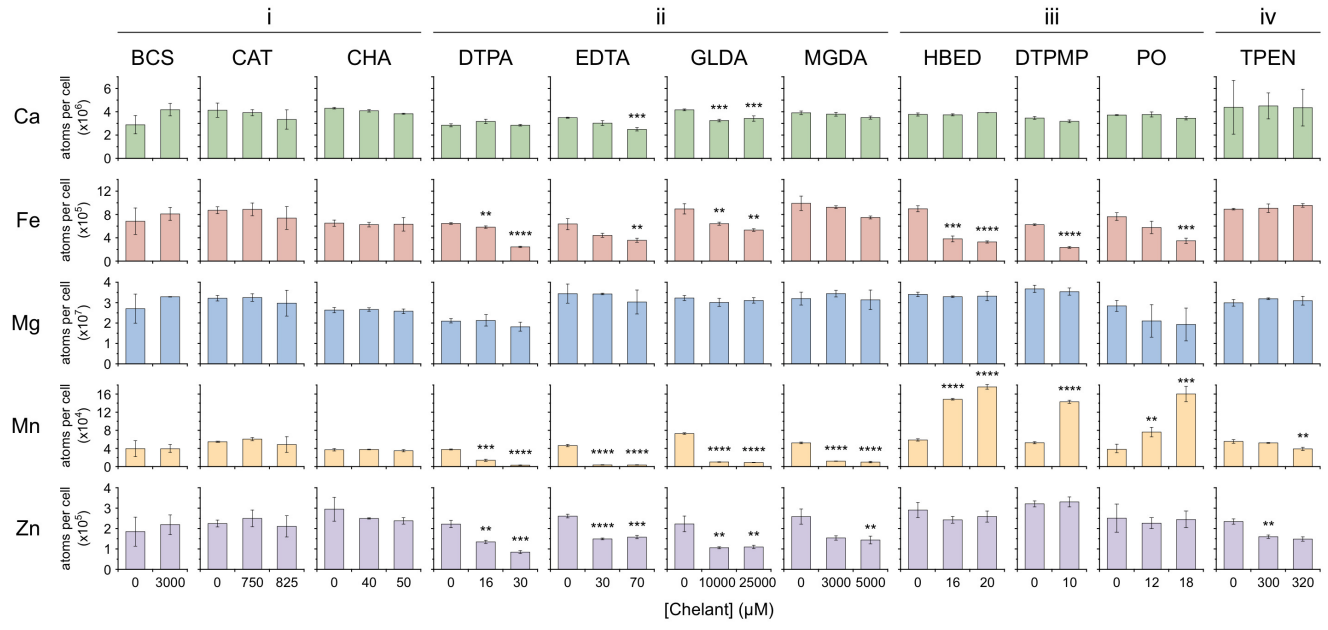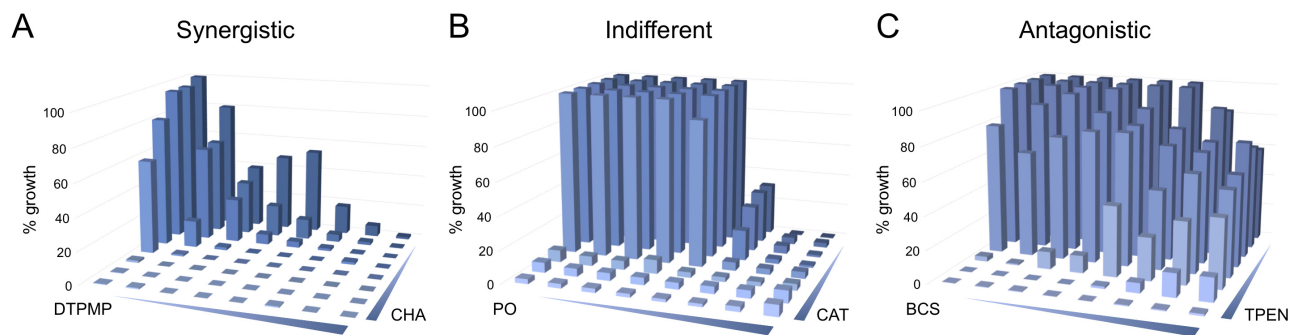
D

	CAT	CHA	DTPA	DTPMP	EDTA	GLDA	HBED	MGDA	PO	TPEN	
	1.50/1.50	2.00/3.00	0.16/0.31	2.00/3.00	1.50/1.50	0.75/2.00	3.00/3.00	1.50/2.00	2.00/2.00	>3.00/5.00	BCS
		1.00/1.00	0.02/0.09	0.06/0.16	0.16/0.19	0.09/0.13	0.53/0.53	0.09/0.16	1.00/1.00	0.16/0.19	CAT
			0.04/0.19	0.04/0.19	0.09/0.16	0.31/0.50	0.25/0.38	0.62/0.75	0.75/1.00	0.09/0.19	CHA
				0.25/0.38	1.50/1.50	0.08/0.09	0.06/0.16	0.09/0.31	0.04/0.15	0.16/0.50	DTPA
					1.25/1.50	2.50/2.50	0.31/0.38	4.00/4.00	0.08/0.09	0.13/0.14	DTPMP
						0.16/0.25	0.75/1.00	0.16/0.16	0.05/0.16	0.75/0.75	EDTA
							0.56/1.00	0.25/0.38	0.75/2.00	1.00/1.00	GLDA
								1.00/2.00	1.00/1.50	0.09/0.13	HBED
									1.00/2.00	0.75/1.00	MGDA
										0.31/0.38	PO

■ Synergistic ≤0.5

■ Indifferent >0.5-≤4.0

■ Antagonistic >4.0

$$\text{FIC index} = \frac{\text{MIC of chelant A in combination}}{\text{MIC of chelant A alone}} + \frac{\text{MIC of chelant B in combination}}{\text{MIC of chelant B alone}}$$

A

● PO 27 µM

Mutant	Growth (%)
ligB	60.01
fepD	60.97/66.36
greB	61.55
fepB	61.81/79.69
tonB	62.34/63.29
fepC	63.62/64.29
fes	67.70
fepG	72.24/81.42
exbD	75.40/82.84
yrdA	75.98
exbB	76.66/77.74
fepA	80.04/85.82
lpp	84.33/84.57
entB	87.22/89.54
proQ	88.71
entA	89.15/92.07
envC	89.99/92.26
entF	90.12/91.52
rfaH	90.27
yciS	90.58
yafN	90.67
tolQ	91.01/94.34
entE	91.06
nlpI	91.11/94.60
ahpC	91.22/91.59
tatC	91.48/92.64
aroC	91.62/93.32
yjeB	91.66/92.78
tolR	91.84/95.88
tatA	92.01
cusR	92.18
rfaG	92.18
aroE	92.25
creB	92.46
fabF	92.64/95.19
endA	92.66
arcA	92.68
tatB	92.90/93.30
yjiC	93.07
cpxA	93.15
rbsB	93.32
ackA	93.43
glnL	93.49
rfaP	93.52
rseA	93.53/95.05
rfaE	93.58
cdd	93.62
sspA	93.70/94.00
fadR	93.76
dusB	93.77

● PO 34 µM

Mutant	Growth (%)
lpp	49.63/56.01
tonB	53.28/54.06
fepD	55.90/57.44
rfaH	57.08
fepC	57.17/57.31
fepB	57.28/59.43
asmA	59.06/59.27
envC	59.33/59.67
tatC	59.47/63.90
dusB	60.00/63.05
fes	60.21
proQ	60.84
yeiH	61.69
fepA	62.02/64.75
yciM	62.15/65.62
yafN	62.35
yraN	62.66
yrbE	63.04/66.20
fepG	63.14/64.56
nlpI	63.32/69.21
ybaK	63.77
tolC	64.08
yjeB	64.28/64.28
bepA	64.39/65.60
ybaZ	64.54
ahpC	64.69/67.40
flhE	64.71
sspA	64.76/66.28
ybgI	64.98
rfaG	65.50
ruvC	65.50
rpiA	65.57
exbD	65.65
gpmI	65.72
cof	65.76
rdgC	65.82
hfq	65.86
tolQ	65.93/68.36
ruvA	65.97/68.81
ptsI	66.19
exbB	66.21/69.35
rnt	66.23
ybgT	66.28/66.91
yegP	66.65
dnaJ	66.66/68.39
rfe	66.71
yeeP	66.72
mrcB	66.80
yadG	66.82
acrB	66.83/68.28

B

■ EDTA 0.5 mM

Mutant	Growth
tatC	-9.52
fepG	-9.23
znuB	-8.85
entA	-7.96
tatB	-7.61
aroG	-6.79
yhaC	-5.80
mepS	-5.60
fes	-5.56
znuA	-5.46
carB	-5.38
aroC	-5.36
entE	-5.28
pyrE	-5.23
aroB	-5.23
ribB	-5.01
purD	-4.93
yaeB	-4.88
yqiC	-4.80
prfA	-4.63
entB	-4.56
aroA	-4.48
citF	-4.40
entF	-4.40
purE	-4.39
pyrC	-4.39
degP	-4.38
aceF	-4.34
entC	-4.29
ninE	-4.22
mdtA	-4.18
lipA	-4.17
allA	-4.07
norW	-3.95
fepC	-3.90
ubiF	-3.88
ryfC	-3.85
tyrR	-3.81
yeaD	-3.76
fkbP	-3.72
sspA	-3.67
yedF	-3.58
yhjJ	-3.52
accD	-3.51
hfq	-3.49
micF	-3.49
ybgT	-3.48
emrD	-3.47
ygbM	-3.44
purM	-3.43

C

Legend:
- Fe^{3+}-enterobactin import
- Enterobactin biosynthesis and export
- Zinc import
- Envelope integrity
- Damage tolerance and stress
- Other

AEM

A

B

C